

FIG. 3. Schematic representation of experimental method. Current supply is triggered by projectile contact with velocity pin. Planar impact occurs between projectile and solenoid when current (hence magnetic field) in solenoid is maximum.

magnetization curve for the independent grain assumption is

$$\begin{aligned} M/M_s &= 1, & x_2 > 1 \\ &= \frac{1}{2}(x_1 + x_2) - \frac{1}{2}(x_1 - 1)^2/(x_1 - x_2), & x_2 \leq 1 \leq x_1, \quad (12) \\ &= \frac{1}{2}(x_1 + x_2), & x_1 < 1, \end{aligned}$$

where

$$x_1 = -(M_s/2b_1e)H_e \text{ and } x_2 = -(M_s/2b_2e)H_e. \quad (13)$$

The predicted magnetization curve for the independent grain theory is qualitatively pleasing for two reasons. First, the magnetization curve tends initially toward saturation more rapidly than is predicted by the interacting grain theory. This behavior is expected because of the excessive energy attributed to the magnetoelastic energy in the interacting grain theory. Secondly, the curve approaches saturation gradually as would be the case if all grains were not forced to saturation simultaneously. In the case of magnetoelastic isotropy ($b_1 = b_2$), the magnetization curve for the independent grain theory is coincident with that of the interacting grain theory. Predicted magnetization curves in YIG for the two theories [Eqs. (5) and (12)] along with those for the $\langle 100 \rangle$ and $\langle 111 \rangle$ problems from the preceding paper are shown in Fig. 2.

III. EXPERIMENTAL METHOD

The experimental method used to obtain shock demagnetization curves and test the theories developed in Sec. II will be briefly described here.²⁶ The theory requires an infinite slab of ferromagnetic material subject to a state of uniaxial strain normal to the plane of the slab and an applied magnetic field in the plane of the slab. This was approximated by a rectangular specimen of polycrystalline yttrium iron garnet. The uniaxial strain was obtained by planar impact of a projectile from a 4-in. gas gun.²⁷ The magnetic field was applied by pulsing a current through a rectangular solenoid enveloping the specimen.

A schematic representation of the experimental procedure is illustrated in Fig. 3. The experimental sequence is as follows: The projectile, travelling at a velocity V triggers the current supply. The subsequent current produces a magnetic field which reaches a maximum and is quasistatic at the time the projectile impacts the target. The current profile is determined by the LCR characteristics of the circuit. The impact produces a strain wave which propagates through the solenoid and into the YIG sample. This sample, initially in magnetic saturation, is demagnetized by the strain wave. The demagnetization develops an emf across the pickup coil, shown schematically in Fig. 3, which is recorded on the monitoring oscilloscopes. Demagnetization of the ferromagnetic material behind the shock wave is determined from these records.

Measurement of the applied magnetic field is made by monitoring the current through a precision noninductive resistor in series with the solenoid. Fields from 200 to 1000 Oe were required in this work. The state of uniaxial strain in the YIG is determined from the measured projectile velocity and the Hugoniot equations of state for the projectile material, intermediate material,^{28,29} and magnetic material³⁰ (Lucite, Lucite, and YIG, respectively, for the first series in Table I). Strains corresponding to about $\frac{1}{3}$ and $\frac{2}{3}$ the Hugoniot elastic limit were produced in the YIG.

The demagnetization records are obtained from the emf developed across a 10-turn pickup coil closely wound around the center of the rectangular YIG specimen. The induced emf is related to the change in magnetization by considering the jump in magnetic flux across a steady-state shock wave. Analysis is similar to that used to obtain mechanical shock-wave jump conditions.³¹ The result is

$$\frac{d\Phi}{dt} = 4\pi bD\Delta M - buH_e, \quad (14)$$

where Φ is the magnetic flux, b is the width of the magnetic specimen and pickup coil, D is the shock velocity, and u is the particle velocity behind the shock wave. In this work, the buH_e contribution was small compared to the first term. $\Delta M = M - M_s$, the change in magnetization per unit initial volume, determines the state of magnetization in the material behind the shock front. In other words, the demagnetization in the material, subject to a given applied field H_e and induced uniaxial strain e , is obtained from the measured emf with Eq. (14) and Faraday's law. A representative demagnetization record is shown in Fig. 4.

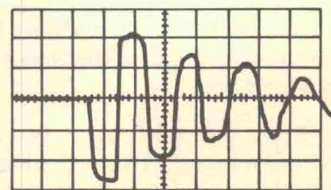


FIG. 4. Oscilloscope record of shock-induced demagnetization in YIG. Periodicity corresponds to reverberation of stress wave in YIG platelet. Time scale is $0.2 \mu \text{ sec/div}$.

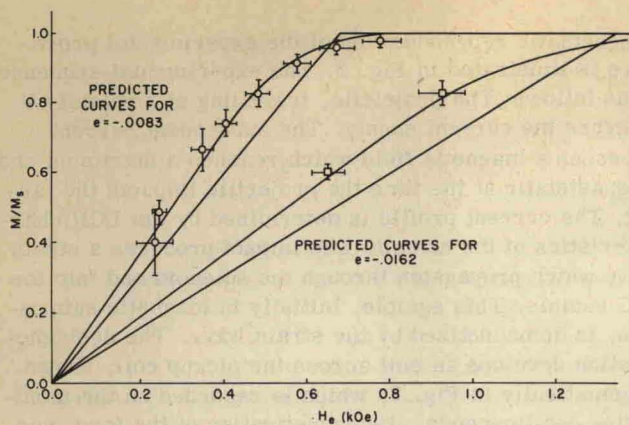


FIG. 5. Experimental data with theoretical magnetization curves for two strain-induced anisotropy fields. Circles correspond to strain of -0.0083 . Squares correspond to strain of -0.0162 . Smooth curves correspond to independent grain theory. Curves with slope discontinuity correspond to interacting grain theory.

The material selected for this study was hot-pressed polycrystalline yttrium iron garnet.³² It was chosen because the magnetoelastic properties are of convenient magnitude for shock-wave investigation. Also this was the material used by Shaner and Royce in earlier investigation of shock-induced demagnetization at high stresses.³ Important points noted during material characterization are the following: Photomicrographs showed the average grain size to be approximately 15μ varying from 5 to 25μ . The grain distribution was visually homogeneous and isotropic throughout the sample; i. e., there was no evidence of mechanical texture created by the hot-pressing process. The porosity was $3.3 \pm 0.5\%$. Pores were highly spherical and observed to occur both intragranularly and at grain boundaries. The specimens were lapped flat and parallel to dimensions of $0.1 \times 1.0 \times 5.0$ cm. Values used for the magnetoelastic constants were $b_1 = 3.5 \times 10^6$ erg/cm³ and $b_2 = 6.9 \times 10^6$ erg/cm³.³⁰ The value used for the theoretically dense saturation magnetization was 133.7 G.³³ The value for the present, slightly porous materials, was 128 G.

IV. EXPERIMENTAL RESULTS

Experimental data are presented in Table I and plotted in Figs. 5 and 6. The strain in the first series corresponds to a longitudinal stress of 22 kbar, the second series to a longitudinal stress of 43 kbar. The Hugoniot elastic limit in YIG is 62 kbar (attributed to Graham).³⁴ Experimental magnetization curves are shown in Fig. 5 along with theoretical curves for the interacting grain and independent grain assumptions. In Fig. 6 the data are plotted as a function of the normalized field H_e/e against which the predicted magnetization curves for any state of strain are self-similar.

It is observed in Figs. 5 and 6 that the two alternative theories differ at most by about 15% in absolute value of magnetization. The measured quantity, however, is the reduction in magnetization or demagnetization. The alternative theories are quite sensitive to this quantity in the upper region of the magnetization curve.

As was mentioned previously, the state of strain in the YIG was determined from equation-of-state knowledge of YIG and the intermediate materials. The accuracy of this method might be questioned since Lucite, a material with known viscoelastic response,²⁸ is used. To alleviate this problem, the propagation distance through Lucite from impact to the YIG interface was kept to a minimum. To test the analysis quartz gauges were substituted at the YIG interface in several experiments. This allowed comparison of calculated strain with measured strain in the quartz. In no case was the difference greater than 4%. The error in the applied field H_e was $\pm 2\%$. Strictly, this was the error in measuring the solenoid current during shock transit. This method was not suspect and no attempt was made to measure the field directly. The horizontal error bars in Figs. 5 and 6 are $\pm 6\%$.

The demagnetization profile in Fig. 3 is observed to exhibit some structure. This structure is typical of all the experimental records. The behavior is due to the finite rise in the strain pulse (~ 50 nsec) and lateral relief waves produced by the finite width of the YIG slabs. An analytic estimate of the structure was made and found consistent with the records. This analysis, however, was not relied on to reduce the error in the experiment. In each profile quite evident extremes occurred to bound the actual demagnetization. These extremes were accepted as error and define the vertical error bars in Figs. 5 and 6 and are the errors quoted in the right-hand column of Table I. This was by far the dominant error. Values for the saturation magnetization in YIG vary from about 128 to 140 G in the literature. The data are not sensitive to this difference.

V. DISCUSSION AND CONCLUSIONS

The data presented in Figs. 5 and 6 support the shock-induced anisotropy mechanism as a contribution to shock demagnetization. It is further concluded that the independent grain assumption provides a better description of the magnetic behavior of polycrystalline ferromagnetic material in the shocked state. Also established

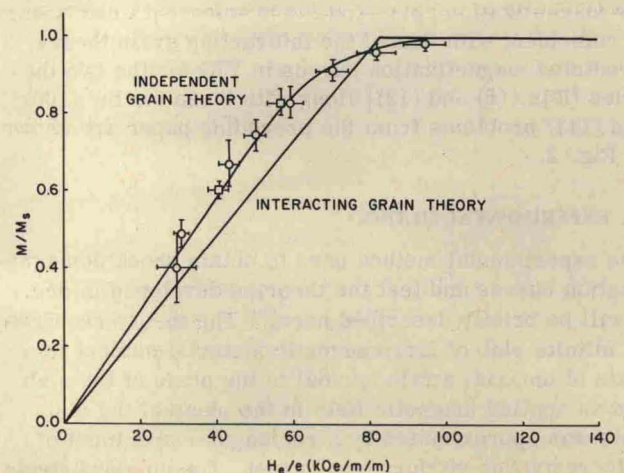


FIG. 6. Data plotted to exhibit theoretically predicted self-similarity of magnetization curves against the parameter H_e/e .